

Effective Biosorption of Phosphate Ions from Aqueous Solution Using Fe(III)-Loaded Carboxyl Functionalized Banana Peels

Pukar Bhattarai¹, Naresh Pant¹, Bhoj Raj Poudel^{2*}, and Ram Lochan Aryal^{1*}

¹Department of Chemistry, Amrit Campus, Tribhuvan University, Kathmandu, Nepal

²Department of Chemistry, Tri Chandra Multiple Campus, Tribhuvan University, Kathmandu, Nepal

*Corresponding E-mail: ram.aryal@ac.tu.edu.np (R.L.A.); bhoj.poudel@trc.tu.edu.np (B.R.P.)

(Received: December 12, 2025, revised: January 23, 2026, accepted: January 25, 2026)

Abstract

Phosphate contamination in water bodies is a major environmental concern due to its role in eutrophication, necessitating the development of low-cost, efficient, and sustainable removal technologies. In this study, an eco-friendly biosorbent was prepared from waste banana peels through saponification followed by Fe(III) loading (Fe(III)-SBP) for effective phosphate ion removal from aqueous solutions. The prepared biosorbent was characterized using FTIR and SEM to confirm functional group modification and surface morphology, while the point of zero charge (pH_{PZC}) was determined to be 6.8. Batch biosorption experiments revealed that phosphate uptake was highly pH-dependent, with a maximum biosorption capacity of 18.51 mg/g at pH 5.34. Equilibrium and kinetic data were best described by the Langmuir isotherm and pseudo-second-order kinetic model, indicating monolayer chemisorption. Competitive ion studies showed negligible interference from chloride and nitrate ions, whereas sulphate and bicarbonate ions significantly inhibited phosphate removal. The adsorbed phosphate was efficiently desorbed using 0.5 M NaOH, demonstrating good regeneration potential of the biosorbent. Overall, the results confirm that Fe(III)-loaded saponified banana peels are an effective, low-cost, and sustainable biosorbent for phosphate removal, highlighting their potential application in wastewater treatment and nutrient pollution control.

Keywords: Saponified banana peels; Fe(III)-SBP; Biosorption; Interfering ions; Phosphate.

Introduction

Phosphate is necessary for the physiological processes of life [1]. It is often present in low concentration in wastewater in the form of phosphate ion, hydrogen phosphate and dihydrogen phosphate [2]. Surface run-offs contribute to an extent of 65% phosphate pollution, industrial waste adds to 25% and domestic and municipal sewages account to 10% [3]. Strict regulatory requirements decreased the permissible level of phosphate concentration (upto 1 mg/L) [4]. The excess discharge of phosphate from the municipal or industrial wastes in the sources of water causes eutrophication [5]. It depletes the level of oxygen which causes reduction in biodiversity [6]. Eutrophication leads to undesirable algal blooms [7].

Phosphate can exist in a variety of ionic species. H_3PO_4 has low affinity for binding sites below pH 2.0 but $H_2PO_4^-$ and HPO_4^{2-} are found in pH range of 2.1 to 7.2. Some of the traditional ways to remove PO_4^{3-} from contaminated water are membrane separation technologies [8], ion exchange [9], reverse osmosis [10]. Likewise there is a growing interest among researchers in using agro-waste products to remove contaminants [11]. Sugarcane bagasse [12], peanut shell [13], apple pomace [14], orange peel [15], litchi seed waste [16], pine bark [17] are some of the agrowastes used for removing pollutants are some of the agrowastes used for removing pollutants. Banana peel is a cellulosic biomass with considerable potential for

functionalization to enhance adsorption sites [18]. Its main structural components include cellulose (7.6–9.6%), hemicellulose (6.4–9.4%), and pectin (10–21%), along with proteins (10.2–12.1%), ash, moisture, and minor constituents [19]. The presence of methyl ester groups of pectin is responsible for chemical modification [20]. Pectin has a carboxy group, which makes it easy to convert into functionalized biosorbent obtained through the saponification process [21]. In this study, Fe(III) ion was selected for loading biosorbent due to their low cost, wide availability, and established use of Fe(III) salts in conventional water and wastewater treatment processes. Unlike Zr(IV) salts, which are relatively expensive and less accessible, Fe(III) compounds are environmentally benign, and non-toxic. These advantages make Fe(III)-loaded biosorbents more suitable for sustainable phosphate removal applications.

Saponification of banana peel generates active carboxylate groups that can coordinate with positively charged metal ions through ligand exchange. In this study, Fe (III) ions were immobilized onto saponified banana peels to develop a low-cost, environmentally friendly biosorbent, and its performance for phosphate removal was systematically evaluated through batch adsorption experiments. Several factors including the influence of pH, biosorption isotherms, kinetic studies and the influence of interfering ions on phosphate biosorption were evaluated.

Materials and Methods

Chemicals

Chemicals like FeCl₃ (70% purity), Ca(OH)₂ (96% purity) and NaH₂PO₄·2H₂O (98% purity) were obtained from Loba Chemical Pvt. Ltd., India. The pH of the solutions was maintained by using HCl and NaOH. All the chemicals used were of analytical grade and were used as received, without any additional purification. All the solutions mentioned above were made in deionized water. The stock solution of phosphate (1000 mg/L) was made by the dissolution of 1.64g of NaH₂PO₄·2H₂O in

1000 mL water. The stock solutions were stored in an airtight bottle from where the working solutions were made by dilution method throughout the experiments.

Preparation of biosorbent material

Raw banana peels were collected from Bhotahity, Kathmandu. They were cut into pieces, sundried for 7 days, grinded and sieved through 150µm. Powder was washed via deionized water to remove contaminants. It was named raw banana peel abbreviated as RBP. 100 g of RBP and 8 g of Ca(OH)₂ powder along with 2 pellets of NaOH were added in a 500 mL beaker. It was stirred in a magnetic stirrer for 24h, filtered and the residue was washed to make neutral. The sample was dried for 24h at 70 °C. The obtained sample is named as saponified banana powder (SBP). Now, 5g of SBP was mixed with 500 mL of 0.01M FeCl₃. pH was maintained at 3 [22]. The mixture of SBP and FeCl₃ was shaken in a flask shaker for 24h. It was filtered and the residue obtained after filtration was washed to make neutral again. The sample was dried at 70 °C for 24h, which is now named as Fe(III)-SBP.

Characterization of the Biosorbent and Biosorption Experiments

Topographical image of RBP, Fe(III)-SBP and Fe(III)-SBP@PO₄ were analyzed by field emission scanning electron microscopy (FE-SEM; JEOL, JSM-6701 F, Japan). Functional groups in RBP, SBP and Fe(III)-SBP were analyzed by Fourier transformed infrared (FTIR) spectroscopy. Dried samples were subjected to FTIR analysis using a Perkin Elmer Spectrometer, version 10.6.2 in the range of 4000-500 cm⁻¹ at a resolution of 4 cm⁻¹. Initial and final concentration of phosphate was evaluated using spectrophotometer (LT-2802, Labtronics, India). Batch adsorption experiments were conducted to evaluate the phosphate removal capacity of Fe(III)-SBP. In each experiment, a known mass of biosorbent (30 mg) was added to 30 mL of phosphate solution with a desired initial concentration. The pH of the solution was adjusted using 0.1

M HCl or 0.1 M NaOH, and the mixture was agitated at 150 rpm using an orbital shaker at room temperature for predetermined contact times. After adsorption, samples were filtered using Whatman No. 42 filter paper, and the residual phosphate concentration was determined by molybdenum blue method using UV-Vis spectrophotometry at 850 nm after complexation with ammonium molybdate and ascorbic acid. The effects of solution pH, initial phosphate concentration, contact time, and competing anions on phosphate uptake were systematically investigated under identical experimental conditions. All experiments were performed in triplicate, and average values were reported. The percentage removal (%A) was calculated using equation (1) [23].

$$\%A = \frac{c_i - c_e}{c_i} \times 100\% \quad (1)$$

where c_i and c_e are the initial concentration and equilibrium concentration of phosphate of a phosphate solution.

Influence of pH, contact time, initial concentration and effect of competing ions were studied by using 10 mg of biosorbent with 10 mL of phosphate. Amount of phosphate biosorbed was calculated by equation (2) [24].

$$q_e = \frac{c_i - c_e}{w} \times V \quad (2)$$

where, q_e is amount of phosphate biosorbed (mg/g), V is the volume of solution (L) and w is the weight of biosorbent (g). The following is the non-linear equation for pseudo-first-order kinetics.

$$q_t = q_e(1 - e^{-K_1 t}) \quad (3)$$

Similarly, the non-linear equation for PSO kinetics is as follows:

$$q_t = \frac{q_e^2 K_2 t}{1 + q_e K_2 t} \quad (4)$$

where q_e and q_t (mg/g) are the adsorption capacity at equilibrium and at time t , respectively; and k_1 , (min^{-1}) and k_2 (g/mg min) are the rate constants of PFO and PSO kinetics, respectively.

Equations (5) and (6) reflect the Langmuir

isotherm's linear and non-linear versions, respectively.

$$\frac{c_e}{q_e} = \frac{1}{q_{\max} \cdot b} + \frac{c_e}{q_{\max}} \quad (5)$$

$$q_e = \frac{q_{\max} \cdot b c_e}{1 + b c_e} \quad (6)$$

where b represents the Langmuir constant, q_{\max} signifies the maximum adsorption capacity.

To calculate pHpzc, 10 mg of Fe(III)-SBP was mixed separately each with 10 mL of 0.01M, 0.05M and 0.1M of NaCl at different pH from 1-12. It was shaking for 24h. The biosorption isotherms of phosphate was analyzed using Langmuir and Freundlich isotherm models. Similarly, kinetic studies were also done [25]. Further, the influence of ions like Cl^- , NO_3^- , CO_3^{2-} , HCO_3^- , SO_4^{2-} were also done.

Desorption Studies

The % desorption of phosphate was obtained from equation (7) [26].

$$\%D = \frac{A_r}{A_b} \times 100\% \quad (7)$$

where A_r and A_b are the amounts of phosphate (mg) bioadsorbed and released, respectively.

Results and Discussion

Characterizations of Biosorbents

The surface morphology of biosorbents was determined by analyzing the scanning electron microscopy (SEM). The surface of RBP is smooth with white patches (**Figure 1(a)**) due to presence of soluble sugars and low molecular weight organic compounds which is anticipated to be leached out after $\text{Ca}(\text{OH})_2$ treatments. Therefore, the surface of Fe(III)-SBP (**Figure 1(b)**) is rough and has uneven protuberances. Similarly, after phosphate was filled in the holes, the surface of Fe(III)-SBP@ PO_4^{3-} has become uniform and smooth (**Figure 1(c)**), which can be properly attributed due to coating of phosphate species onto Fe(III)-SBP surface.

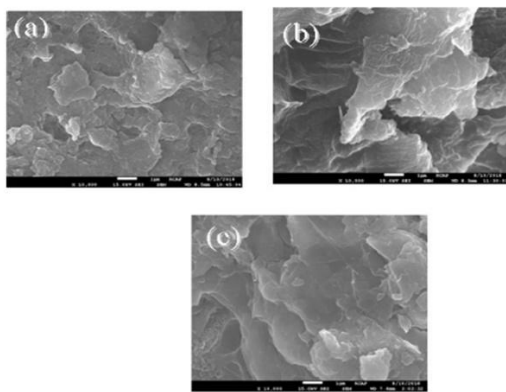


Figure 1: SEM images of a) RBP, b) Fe(III)-SBP and c) Fe(III)-SBP@PO₄

FTIR spectroscopy was employed to investigate the surface functional groups of RBP, saponified banana peel (SBP), Fe(III)-SBP, and phosphate-loaded Fe(III)-SBP (**Figure 2**), and to elucidate the adsorption mechanism. The FTIR spectrum of RBP exhibited a broad band around 3348 cm⁻¹ corresponding to O–H stretching vibrations of hydroxyl groups. The peak observed near 2923 cm⁻¹ is attributed to aliphatic C–H stretching, while the band around 1735 cm⁻¹ corresponds to C=O stretching of ester and carboxylic acid groups [27]. In FTIR spectrum of Fe(III)-SBP, significant changes were observed. The carboxylate stretching bands showed noticeable shifts and reduced intensity, indicating coordination between Fe(III) ions and the carboxylate functional groups of the biosorbent. Additionally, the broad O–H stretching band became less intense, suggesting involvement of hydroxyl groups in Fe(III) binding. These changes confirm the successful loading of Fe(III) ions onto the SBP surface. After phosphate adsorption, further spectral changes were evident. The Fe–carboxylate related bands showed additional shifts, and new bands appeared in the region of 1016 and 1242 cm⁻¹, which are characteristic of P–O stretching vibrations of phosphate species. This suggests that phosphate adsorption occurs predominantly through ligand exchange and inner-sphere complex

formation, where phosphate ions replace surface hydroxyl or coordinated water molecules bound to Fe(III) [28].

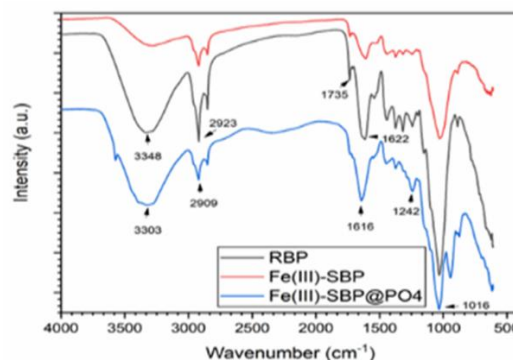


Figure 2: FTIR spectra of RBP, Fe(III)-SBP and Fe(III)-SBP@PO₄

Surface Charge of the Biosorbent

The point of zero charge (pH_{pzc}) was evaluated by plotting the graph between initial pH and ΔpH as shown in **Figure 3**. The pH_{pzc} value was found at 6.8 from the graph. At the value of pH_{pzc}, the surface charge of biosorbent becomes neutral, due to which the phosphate anions of aqueous solutions substitute the hydroxyl groups by ligand exchange mechanism. On the other hand, when the pH is below pH_{pzc}, the surface charge of biosorbent becomes positive due to protonation phenomenon. So, the biosorption of phosphate anion favors at lower pH because of the electrostatic force of attraction between the phosphate anion and surface of biosorbent [29].

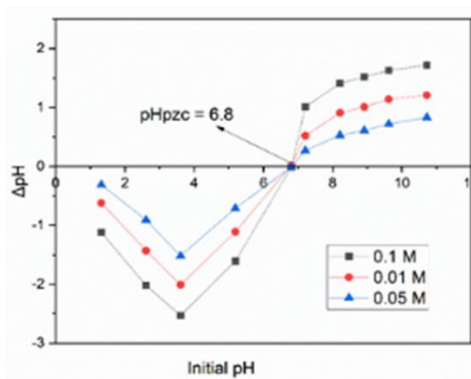


Figure 3: Determination of point zero charge (pH_{pzc}) for Fe(III)-SBP

Influence of pH

The biosorption of phosphate anion is influenced by surface charge of biosorbent. The biosorption performance of RBP and Fe(III)-SBP under varying pH is shown in **Figure 4**, which demonstrates that the percentage of phosphate biosorbed on to RBP increased from 3.6% at pH 1.5 to 19% at pH 5.34 whereas Fe(III)-SBP exhibited greater efficacy for the biosorption of phosphate from 7.06% at pH 1.5 to 88.80% at pH 5.34. After the optimum pH, biosorption process decreased gradually. At this pH, the biosorption took place through electrostatic interaction as well as ligand exchange mechanism, but at higher pH, the electrostatic repulsion between hydroxyl ions and phosphate ions have reduced the biosorption process [30].

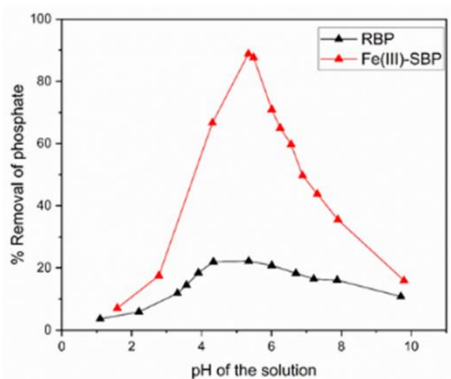


Figure 4: Influence of pH for the biosorption of phosphate onto Fe(III)-SBP

Influence of Contact Time

The findings of the kinetic studies of Fe(III)-SBP at pH 5.34 are given in **Figure 5**. **Figure 5 (a)** showed the progressive rise in the phosphate biosorption, then slowed down and finally achieved plateau at 6 h. **Figure 5 (b)** showed the non-linear plot of pseudo-first-order (PFO) and pseudo-second-order (PSO) kinetic model [31]. PSO data are in line with experimental data rather than the PFO data. Similarly, **Figure 5 (c)** and **Figure 5 (d)** showed separate linear plot of PFO and PSO respectively. It showed PSO kinetic model better fit because coefficient of determination of

PSO ($R^2 = 0.98$) is greater than the coefficient of determination of PFO ($R^2 = 0.91$). Likewise, the value of q_e calculated from PSO (4.032 mg/g) is close to observed q_e (3.91 mg/g). Hence, phosphate biosorption followed PSO kinetics which confirms the chemisorption process is involved in this biosorption phenomenon [32]. The kinetic parameters were tabulated in **Table 1**.

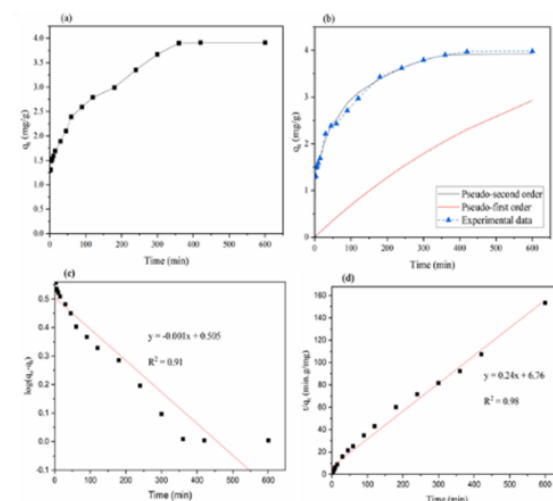


Figure 5: Biosorption of phosphate onto Fe(III)-SBP (a) Influence of contact time (b) Non-linear kinetics of phosphate biosorption onto Fe(III)-SBP (c) Plot of pseudo-first-order and (d) pseudo-second-order model

Table 1: Kinetic parameters for the biosorption of phosphate onto Fe(III)-SBP

Order	R^2	q_e (exp) (mg/g)	q_e (cal) (mg/g)	k_1 (min^{-1})	k_2 (mg/g/min)
PSO	0.989	3.91	4.0	-	0.009
PFO	0.912	3.91	0.505	0.002	-

Biosorption Isotherm Studies

Figure 6 (a) showed the phosphate biosorption increases at lower concentration then slowed down and attains a plateau region. **Figure 6 (b)** showed that experimental data is in line with the Langmuir isotherm model. Similarly, separate Langmuir [33] and Freundlich isotherm model [34] were plotted in the graph which have the coefficient of determination ($R^2 = 0.982$) and ($R^2 = 0.91$) respectively. It showed Langmuir model best fit

the data. Likewise, maximum biosorption capacity (q_{max}) was calculated to be 18.51 mg/g (Langmuir) which is similar to the experimental data (17.31 mg/g). Hence, phosphate biosorption followed Langmuir isotherm model which confirms monolayer biosorption is involved. The evaluated values of isotherm parameters were listed in **Table 2**.

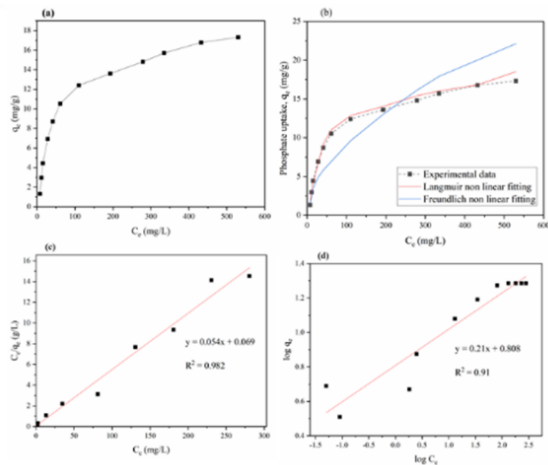


Figure 6: (a) Influence of initial concentration (b) non-linear isotherm of phosphate biosorption onto Fe(III)-SBP (c) Langmuir isotherm (d) Freundlich isotherm

Table 2: Isotherm parameters for the phosphate biosorption onto Fe(III)-SBP

Langmuir Isotherm			Freundlich Isotherm		
q_{max} (mg/g)	b (L/mg)	R^2	K_F	1/n	R^2
18.51	0.78	0.98	5.5	0.24	0.91

Table 3: Comparison of uptake capacity of Fe(III)-SBP with other biosorbents

S.N.	Biosorbent	q_{max} (mg/g)	Reference
1	Zr(IV)-SOW	13.94	[35]
2	Zr(IV)-SWR	27.63	[21]
3	Zr-MCM 41	3.36	[36]
4	Modified almond wooden shell	22.73	[37]
5	La(III)-modified Pine needles	4.8	[38]
6	Fe-loaded activated	2.87	[39]

	carbon		
7	Zr(IV)-loaded Okara	44.13	[40]
8	Zr(IV)-loaded apple peels	20.35	[41]
9	La-incorporated porous zeolite	17.2	[42]
10	Fe(III)-loaded pomegranate peel	99.30	[43]
11	Fe(III)-SBP	18.51	This study

Influence of Interfering Anions

The presence of coexisting anions in aqueous solutions can significantly influence phosphate adsorption. In our study, Cl^- , HCO_3^- and NO_3^- had negligible effects, whereas SO_4^{2-} significantly inhibited adsorption. This difference can be explained by the stronger affinity of multivalent anions for Fe(III) centers. SO_4^{2-} compete with phosphate ions for coordination to surface-bound Fe(III) sites, reducing available binding sites. In contrast, monovalent anions interact weakly with Fe(III), resulting in minimal interference. These results highlight the selectivity of Fe(III)-SBP toward phosphate over common monovalent ions [29,44,45].

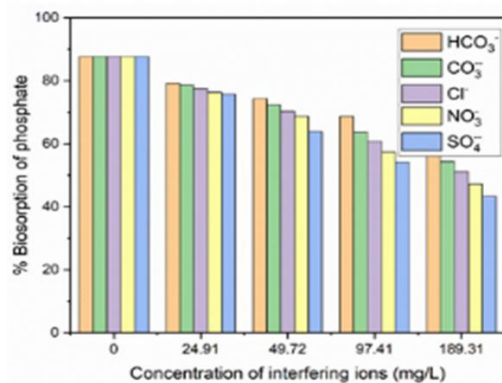
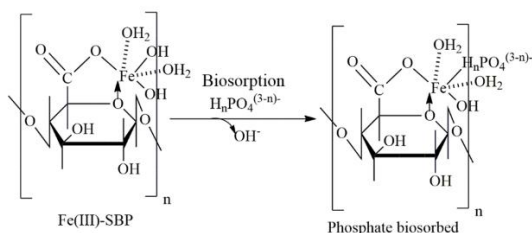


Figure 7: Influence of interfering anions in the biosorption of phosphate onto Fe(III)-SBP

Phosphate Biosorption Mechanism

Scheme 1 showed Fe(III)-SBP and phosphate biosorbed Fe(III)-SBP. Fe(III)-SBP undergoes ligand exchange mechanism. (OH) group of Fe(III)-SBP is replaced by $H_nPO_4^{(3-n)-}$

which is present in the aqueous solution [46].



Scheme 1: Inferred mechanism of phosphate biosorption onto Fe(III)-SBP biosorbent

Desorption Studies

NaOH of 0.01, 0.1, 0.2, 0.5 and 1M were used, where phosphate desorption increased from 53.21% to 93.34% from 0.01 to 0.5M. However, desorption of biosorbed phosphate decreased with 1M NaOH because it ruptured the surfaces of Fe(III)-SBP [21].

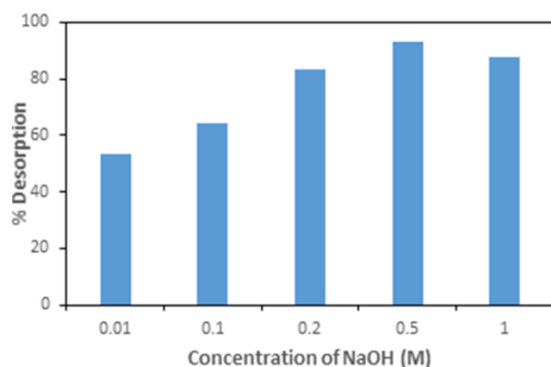
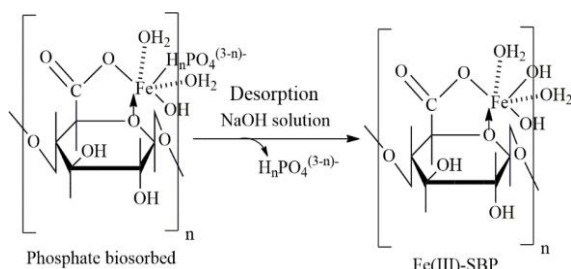


Figure 8: Desorption of phosphate biosorbed Fe(III)-SBP as a function of NaOH concentration.



Scheme 2: Inferred mechanism of phosphate desorption using NaOH solution.

Scheme 2 shows the biosorbed phosphate anion can be easily desorbed with NaOH by the ligand exchange mechanism between the biosorbed phosphate anions and high concentration of OH⁻ ions present in the solution [21].

Conclusions

Phosphate biosorption from aqueous solution was investigated using Fe(III)-SBP as the biosorbent. To prepare Fe(III)-SBP, banana peel powder was saponified with Ca(OH)₂ and then loaded Fe(III). SEM analysis showed the morphology of Fe(III)-SBP before and after biosorption. FTIR analysis indicated the principal role of carboxyl functional group for biosorption. The pH_{PZC} was determined at 6.8. The phosphate uptake (q_{max}) was found to be 18.51 mg/g. Kinetic analysis showed that PSO kinetic model best suited the data. Ions like Cl⁻, NO₃⁻, CO₃²⁻ and HCO₃⁻ have no appreciable influence but SO₄²⁻ has maximum interference. Using 0.5M NaOH, the biosorbed phosphate was successfully eluted. Compared to reported biosorbents, Fe(III)-SBP has superior phosphate biosorption performance. The experimental findings revealed that Fe(III)-SBP can be efficient and low-cost material for phosphate biosorption.

Acknowledgements

The authors wish to thank Dr. Deval Prasad Bhattarai for UV-vis spectrophotometer. The first author (P. Bhattarai) acknowledges funding from National Youth Council.

Author's contribution statement

P. Bhattarai: Experimental, Methodology, Data curation, Validation, Writing-original draft, **N. Panta:** Data curation, Validation, Formal analysis, Writing-original draft preparation, **B. R. Poudel; R. L. Aryal:** Conceptualization, Methodology, Software, Validation, Formal analysis, Writing-review and editing, and Supervision.

Conflict of interest

The authors do not have any conflict of interest pertinent to this work.

Data availability statement

The data that supports the findings of this study can be made available from the corresponding author, upon reasonable request.

References

- J. Dong, G. Ma, L. Sui, M. Wei, V. Satheesh, R. Zhang, S. Ge, J. Li, T.E. Zhang, C. Wittwer, H.J. Jessen, H. Zhang, G.Y. An, D.Y. Chao, D. Lui, and M. Lei, Inositol pyrophosphate insp8 acts as an intracellular phosphate signal in Arabidopsis, *Molecular Plant*, 2019, 12(11), 1463-1473. (doi.org/10.1016/j.molp.2019.08.002)
- R. Glaum and T. Staffel, 6.2 Phosphates, R. Pöttgen, T. Jüstel and C. A. Strassert (eds.), Volume 2 From Energy Storage to Photofunctional Materials, De Gruyter, 2023, Germany. (doi.org/10.1515/9783110798890-010)
- A. Shrestha, B.R. Poudel, M. Silwal, and M. R. Pokhrel, Adsorptive removal of phosphate onto iron loaded litchi chinensis seed waste, *Journal of Institute of Science and Technology*, 2018, 23(1), 81-87. (doi.org/10.3126/jist.v23i1.22200)
- A. A. S. Saleh, N. Ibrahim, N. R. Awang, and N. A. Akbar, Characteristics study of ammonia-n and phosphorus in sewage wastewater effluent: a case study of Alkhumrah, Jeddah Wastewater Treatment Plant, *In IOP Conference Series: Earth and Environmental Science*, 2021, 842(1), 012034. (doi:10.1088/1755-1315/842/1/012034)
- M. Preisner, E. Neverova-Dziopak, and Z. Kowalewski, Mitigation of eutrophication caused by wastewater discharge: A simulation-based approach, *Ambio*, 2021, 50(2), 413-424. (doi.org/10.1007/s13280-020-013)
- C. E. Boyd, Eutrophication, Water Quality: An Introduction, 2020, 311-322. (doi.org/10.1007/978-3-030-23335-8_15)
- W. A. Wurtsbaugh, H. W. Paerl, and W. K. Dodds, Nutrients, eutrophication and harmful algal blooms along the freshwater to marine continuum, *Wiley Interdisciplinary Reviews: Water*, 2019, 6(5), e1373. (doi.org/10.1002/wat2.1373)
- X. Li, S. Shen, Y. Xu, T. Guo, H. Dai, and X. Lu, Application of membrane separation processes in phosphorus recovery: A review. *Science of the Total Environment*, 2021, 767, 144346. (doi.org/10.1016/j.scitotenv.2020.144346)
- K. Zhou, B. Wu, X. Chai, and X. Dai, Co-immobilization of clinoptilolite and nanostructured hydrated ferric-zirconium binary oxide via polyvinyl alcohol-alginate covalent cross-linking for simultaneous deep removal of aqueous low-level nitrogen and phosphorus, *Arabian Journal of Chemistry*, 2021, 14(10), 103354. (doi.org/10.1016/j.arabjc.2021.103354)
- M. Gomelya, T. Shabliy, I. Radovenchyk, and A. Vakulenko, Determining the efficiency of reverse osmosis in the purification of water from phosphates, *Journal of Ecological Engineering*, 2023, 24(2). (doi.org/10.12911/22998993/157023)
- R. Shrivastava, and N. K. Singh, Agro-wastes sustainable materials for wastewater treatment: Review of current scenario and approaches for India, *Materials Today: Proceedings*, 2022, 60, 552-558. (doi.org/10.1016/j.matpr.2022.01.460)
- W. S. Carvalho, D. F. Martins, F. R. Gomes, I. R. Leite, L. G. da Silva, R. Ruggiero, and E. M. Richter, Phosphate adsorption on chemically modified sugarcane bagasse fibres, *Biomass and bioenergy*, 2011, 35(9), 3913-3919. (doi.org/10.1016/j.biombioe.2011.06.014)
- K. W. Jung, M. J. Hwang, K. H. Ahn, and Y. S. Ok, Kinetic study on phosphate removal from aqueous solution by biochar derived from peanut shell as renewable adsorptive media, *International Journal of Environmental Science and Technology*, 2015, 12, 3363-3372. (doi.org/10.1007/s13762-015-0766-5)
- K. P. Thangavelu, B. Tiwari, J. P. Kerry, C. K. McDonnell, and C. Álvarez, Phosphate replacing potential of apple pomace and coffee silver skin in Irish breakfast sausage using a mixture design approach, *Meat Science*, 2022, 185, 108722. (doi.org/10.1016/j.meatsci.2021.108722)
- Z. Chen, Y. Wu, Y. Huang, L. Song, H. Chen, S. Zhu, and C. Tang, Enhanced adsorption of phosphate on orange peel-based biochar activated by Ca/Zn composite: Adsorption efficiency and mechanisms, *Colloids and Surfaces A: Physicochemical and Engineering Aspects*, 2022, 651, 129728. (doi.org/10.1016/j.colsurfa.2022.129728)
- A. Shrestha, B. R. Poudel, M. Silwal, M. R.

- Pokhrel, Adsorptive removal of phosphate onto iron loaded litchi chinensis seed waste, *Journal of Institute of Science and Technology*, 2018, 23(1), 81-87. (doi.org/10.3126/jist.v23i1.22200)
17. A. Karachalios, and M. Wazne, Phosphate removal from water by modified pine bark using ionic liquid analog, *Desalination and Water Treatment*, 2015, 54(7), 1881-1892. (doi.org/10.1080/19443994.2014.893209)
 18. K. G. Akpomie, and J. Conradie, Banana peel as a biosorbent for the decontamination of water pollutants, A review. *Environmental Chemistry Letters*, 2020, 18(4), 1085-1112. (doi.org/10.1007/s10311-020-00995-x)
 19. R. L. Aryal, B.R. Poudel, M. R. Pokhrel, H. Paudyal, and K. N. Ghimire, Effectiveness of Zr (IV)-Loaded Banana Peels Biomass for the Uptake of Fluoride Anion from Water, *Journal of Institute of Science and Technology*, 26(2), 2021, 67-78. (doi.org/10.3126/jist.v26i2.41436)
 20. R. Wang, R. Liang, T. Dai, J. Chen, X. Shuai, and C. Liu, Pectin-based adsorbents for heavy metal ions: A review, *Trends in Food Science and Technology*, 2019, 91, 319-329. (doi.org/10.1016/j.tifs.2019.07.033)
 21. R. L. Aryal, K. P. Bhurtel, B. R. Poudel, M. R. Pokhrel, H. Paudyal, K. N. Ghimire, Sequestration of phosphate from water onto modified watermelon waste loaded with Zr (IV), *Separation Science and Technology*, 2022, 57(1), 70-82. (doi.org/10.1080/01496395.2021.1884878)
 22. M. R. Pokhrel, B. R. Poudel, R. L. Aryal, H. Paudyal, and K. N. Ghimire, Removal and recovery of phosphate from water and wastewater using metal-loaded agricultural waste-based adsorbents: a review, *Journal of Institute of Science and Technology*, 2019, 24(1), 77-89. (doi.org/10.3126/jist.v24i1.24640)
 23. B. R. Poudel, R. L. Aryal, S. Bhattarai, A. R. Koirala, S. K. Gautam, K. N. Ghimire, and M. R. Pokhrel, Agro-waste derived biomass impregnated with TiO₂ as a potential adsorbent for removal of As (III) from water, 2020, *Catalysts*, 10(10), 1125. (dx.doi.org/10.3390/catal10101125)
 24. B. R. Poudel, R.L. Aryal, S. K. Gautam, K. N. Ghimire, H. Paudyal, and M. R. Pokhrel, Effective remediation of arsenate from contaminated water by zirconium modified pomegranate peel as an anion exchanger, *Journal of Environmental Chemical Engineering*, 2021, 9(6), 106552. (doi.org/10.1016/j.jece.2021.106552)
 25. R. L. Aryal, A. Thapa, B. R. Poudel, M. R. Pokhrel, B. Dahal, H. Paudyal, K. N. Ghimire, Effective biosorption of arsenic from water using La (III) loaded carboxyl functionalized watermelon rind, *Arabian Journal of Chemistry*, 2022, 15(3), 103674. (doi.org/10.1016/j.arabjc.2021.103674)
 26. R. Rai, R. L. Aryal, H. Paudyal, S. K. Gautam, K. N. Ghimire, M. R. Pokhrel, and B. R. Poudel, Acid-treated pomegranate peel; An efficient biosorbent for the excision of hexavalent chromium from wastewater, *Heliyon*, 2023, 9(5). (doi.org/10.1016/j.heliyon.2023.e15698)
 27. R. L. Aryal, B. R. Poudel, M. R. Pokhrel, H. Paudyal, and K. N. Ghimire, Effectiveness of Zr (IV)-Loaded Banana Peels Biomass for the Uptake of Fluoride Anion from Water, *Journal of Institute of Science and Technology*, 2021, 26(2), 67-78. (doi.org/10.3126/jist.v26i2.41436)
 28. B. R. Poudel, D. S. Ale, R. L. Aryal, K. N. Ghimire, S. K. Gautam, H. Paudyal, H., M. R. Pokhrel, Zirconium modified pomegranate peel for efficient removal of arsenite from water, *Bibechana*, 2022, 19(1-2), 1-13. (doi.org/10.3126/bibechana.v19i1-2.45943)
 29. N. D. Suzaimi, P. S. Goh, N. A. N. N. Malek, J. W. Lim, and A. F. Ismail, Enhancing the performance of porous rice husk silica through branched polyethyleneimine grafting for phosphate adsorption, *Arabian Journal of Chemistry*, 2009, 13(8), 6682-6695. (doi.org/10.1016/j.arabjc.2020.06.023)
 30. H. Paudyal, B. Pangeni, K. Inoue, H. Kawakita, K. Ohto, K. N. Ghimire, and S. Alam, Adsorptive removal of trace concentration of fluoride ion from water by using dried orange juice residue, *Chemical Engineering Journal*, 2013, 223, 844-853. (doi.org/10.1016/j.cej.2013.03.055)
 31. Y. S. Ho, and G. McKay, Sorption of dye from aqueous solution by peat. *Chemical Engineering Journal*, 1998, 70(2), 115-124.

- (doi.org/10.1016/S0923-0467(98)00076-1)
32. G. Markou, D. Mitrogiannis, K. Muylaert, A. Çelekli, and H. Bozkurt, Biosorption and retention of orthophosphate onto Ca (OH)₂-pretreated biomass of Phragmites sp. *Journal of Environmental Sciences*, 2016, 45, 49-59. (doi.org/10.1016/j.jes.2015.12.009)
 33. I. Langmuir, The constitution and fundamental properties of solids and liquids. Part I. Solids, *Journal of the American Chemical Society*, 1916, 38(11), 2221-2295. (doi.org/10.1021/ja02268a002)
 34. H. Freundlich, About adsorption in solutions, *Journal of Physical Chemistry*, 1907, 57(1), 385-470. (doi.org/10.1515/zpch-1907-5723)
 35. B. K. Biswas, K. Inoue, K. N. Ghimire, H. Harada, K. Ohto, and H. Kawakita, Removal and recovery of phosphorus from water by means of adsorption onto orange waste gel loaded with zirconium, *Bioresource Technology*, 2008, 99(18), 8685-8690. (doi.org/10.1016/j.biortech.2008.04.015)
 36. W. Jutidamrongphan, K. Y. Park, S. Dockko, J. W. Choi, and S. H. Lee, High removal of phosphate from wastewater using silica sulfate, *Environmental Chemistry Letters*, 2012, 10, 21-28. (doi.org/10.1007/s10311-011-0323-5)
 37. B. Faraji, M. Zarabi, and Z. Kolahchi, Phosphorus removal from aqueous solution using modified walnut and almond wooden shell and recycling as soil amendment, *Environmental Monitoring and Assessment*, 2020, 192(6), 373. (doi.org/10.1007/s10661-020-08326-x)
 38. X. Wang, Z. Liu, J. Liu, M. Huo, H. Huo, and W. Yang, Removing phosphorus from aqueous solutions using lanthanum modified pine needles, *PLoS One*, 2015, 10(12), e0142700. (doi.org/10.1371/journal.pone.0142700)
 39. J. C. A. Braun, C.E. Borba, M. Godinho, D. Perondi, J. M. Schontag, and B. M. Wenzel, Phosphorus adsorption in Fe-loaded activated carbon: Two-site monolayer equilibrium model and phenomenological kinetic description, *Chemical Engineering Journal*, 2019, 361, 751-763. (doi.org/10.1016/j.cej.2018.12.073)
 40. A. T. Nguyen, H. H. Ngo, W. S. Guo, J. L. Zhou, J. Wang, H. Liang, and G. Li, Phosphorus elimination from aqueous solution using 'zirconium loaded okara' as a biosorbent. *Bioresource Technology*, 2014, 170, 30-37. <https://doi.org/10.1016/j.biortech.2014.07.069>
 41. R. Mallampati, and S. Valiyaveetil, Apple Peels - a Versatile Biomass for Water Purification? *ACS Applied Materials and Interfaces*, 2013, 5(10), 4443-4449. <https://doi.org/10.1021/am400901e>
 42. Y. He, H. Lin, Y. Dong, and L. Wang, Preferable Adsorption of Lanthanum-incorporated Phosphate Porous Using Zeolite: Characteristics and Mechanism. *Applied Surface Science*, 2017, 426, 995-1004. <https://doi.org/10.1016/j.apsusc.2017.07.272>
 43. N. Bashyal, S. Aryal, R. Rai, P. C. Lohani, S. K. Gautam, M. R. Pokhrel, and B. R. Poudel, Effective biosorption of phosphate from water using Fe (III)-Loaded pomegranate peel, *Chemical and Biochemical Engineering Quarterly*, 2023, 37(2), 67-77. <https://doi.org/10.15255/CABEQ.2022.2174>
 44. J. Lin, S. He, Y. Zhan, and H. Zhang, Evaluation of phosphate adsorption on zirconium/magnesium-modified bentonite. *Environmental Technology*, 2020, 41(5), 586-602. (doi.org/10.1080/09593330.2018.1505966)
 45. A. Nakarmi, S. E. Bourdo, L. Ruhl, S. Kanel, M. Nadagouda, P. K. Alla, and T. Viswanathan, Benign zinc oxide betaine-modified biochar nanocomposites for phosphate removal from aqueous solutions, *Journal of Environmental Management*, 2020, 272, 111048. (doi.org/10.1016/j.jenvman.2020.111048)
 46. H. Paudyal, B. Pangeni, K. Inoue, H. Kawakita, K. Ohto, H. Harada, and S. Alam, Adsorptive removal of fluoride from aqueous solution using orange waste loaded with multi-valent metal ions, *Journal of Hazardous Materials*, 2011, 192(2), 676-682. (doi.org/10.1016/j.jhazmat.2011.05.070)